Fault Tolerant Longitudinal Aircraft Control using Nonlinear Integral Sliding Mode

Halim Alwi and Christopher Edwards

Abstract

This paper proposes a novel nonlinear fault tolerant scheme for longitudinal control of an aircraft system, comprising an integral sliding mode control allocation scheme and a backstepping structure. In fault free conditions, the closed loop system is governed by the backstepping controller and the integral sliding mode control allocation scheme only influences the performance if faults/failures occur in the primary control surfaces. In this situation the allocation scheme redistributes the control signals to the secondary control surfaces and the scheme is able to tolerate total failures in the primary actuator. A backstepping scheme taken from the existing literature is designed for flight path angle tracking (based on the nonlinear equations of motion) and this is used as the underlying baseline controller in nominal conditions. The efficacy of the scheme is demonstrated using a high fidelity aircraft benchmark model. Excellent results are obtained in the presence of plant/model uncertainty in both fault-free and faulty conditions.

Keyword: Fault tolerant control (FTC), integral sliding mode (ISM) control.

I. Introduction

The study of fault tolerant control (FTC) has received much attention in the last decade. Many different schemes have been proposed, ranging from active to passive control methods [1], with applications running the gamut from large scale petrochemical plants to automotive and aerospace systems [2]. The work in [1], [2], [3], [4] provides an excellent literature review on the different schemes used for FTC including different applications; however, research into FTC has been significantly driven by problems encountered in the safety critical aerospace industry. This is due to the practical requirement for increasing safety as well as lowering operational costs. Many different FTC methods, specific to aircraft applications, have been proposed including linear approaches (e.g. $\mathcal{H}_\infty$ [5], LQG [6], model-following [7], multiple model [8], model predictive control [9]), and nonlinear approaches (e.g. nonlinear dynamic inversion [10], backstepping [11], neural networks [12], sliding mode [13]). Some of these methods have attracted the attention of industry and have been further tested and evaluated in order to assess their potential for future applications and implementations on aircraft (see for example the European study on state-of-the-art FTC by the GARTEUR AG-16 group [14] and the recent ADDSAFE project [15]). However many of these proposed FTC schemes are based on linear plant representations and are therefore only valid in the vicinity of the designed trim point. Therefore, one of the main challenges for practical implementation, especially for aircraft, is to ensure good performance for a wide range of operating conditions. Some of the linear based designs can be extended to handle variations in operating conditions (see for example, gain scheduling and linear parameter varying (LPV) schemes [16], [17]), but direct nonlinear methods such as nonlinear dynamic inversion (NDI) and backstepping provide equally viable alternatives – with many benefits compared to the extended linear cases. One obvious benefit is the direct exploitation of the well known aircraft equations of motion, which provide good and consistent performance throughout the flight envelope.

One of the promising schemes to emerge for aircraft FTC in recent decades is sliding mode control (SMC). The interest stems from the inherent robustness properties of SMC to 'matched uncertainty' [18], [19] – which includes as a special case faults

H. Alwi and C. Edwards are with the Structures and Dynamics Group, College of Engineering, Mathematics and Physical Sciences, University of Exeter, EX4 4QF, UK. h.alwi@exeter.ac.uk, C.Edwards@exeter.ac.uk

which occur in the input channels of the system i.e. faulty actuators. Despite the potential and promising features of these controllers, many of the existing schemes are still based on linearizations of the plant dynamics about a specific operating condition [20], [21]. In this paper a backstepping approach will be adopted in order to deal with variations in the operating conditions in conjunction with sliding mode control allocation.

In this paper, a specific type of sliding mode control will be considered – so-called integral sliding mode (ISM) control [22]. In comparison with conventional sliding mode schemes, an ISM has no reaching phase [18], [19], and therefore robustness is guaranteed for all time. A number of authors have applied sliding mode techniques to the design of flight control laws: see for example [23], [24], [25], [26]. However many of these papers do not consider the fault tolerant control aspects and focus instead on the robustness properties introduced by the sliding modes. Some notable exceptions are [27], [28]. However the scheme (especially in [28]) can only deal with partial actuator faults and cannot cope with the problem of total actuator failure. This will be a key facet of the proposed scheme introduced in this paper. The combination of ISM concepts together with a form of control allocation will allow a certain class of total failures to occur, which cannot be achieved by an ISM scheme alone.

The main contributions of the scheme proposed in this paper compared to the existing ISM FTC literature are the following. Firstly, unlike existing sliding mode FTC schemes, the scheme proposed in this paper can handle both actuator faults and failures. This is achieved by incorporating control allocation in order to automatically redistribute the control signals to redundant healthier actuators when faults/failures occur. The combination of the backstepping ISM structure with control allocation, allows the same controller to be used in both the nominal and faulty situations and distinguishes this paper from existing backstepping based SMC/ISM schemes for nonlinear systems (see for examples [29], [30], [31]).

Secondly, since the scheme automatically redistributes the control signals in the event of a fault/failure scenario, the proposed scheme does not require any bumpless transfer mechanism [32], [33] which typically must be used when switching from a fault free controller to the FTC controller. Note that the choice of allocation matrix is novel compared to the one in [20], [21], and takes into account the structure of the aircraft equations of motion considered in this paper. This structure has been exploited to the full. The approach proposed in this paper also takes into account the effect of errors associated with the estimation of the effectiveness matrices, that model the effect of the fault, and provides a bespoke analysis which exploits the structure to reduce conservatism. The specific bounds obtained here are not obtained as a special case of the linear systems in [21]. Compared with the existing schemes designed from linear models, the underlying nonlinear backstepping controller has guaranteed levels of stability and performance for a wide range of flight conditions. Furthermore, the backstepping design from [11], [34] has a simple structure and does not require exact detailed knowledge of the aircraft dynamics (e.g. the coefficient of forces and moments). This proposed scheme is attractive and convenient in comparison to [35], [36] as the tuning parameters are only associated with the nonlinear modulation gain for the sliding mode controller.

II. Nonlinear Aircraft Model

In this paper, the longitudinal motion rigid aircraft will be considered. Such model is typically given by four differential equations [37], [38]:

$$\dot{V}_{tas} = \frac{1}{m}\left(-D + T_n\cos(\alpha+\sigma_T) - mg\sin\gamma\right) \quad (1)$$

$$\dot{\alpha} = \frac{1}{mV_{tas}}\left(-L - T_n\sin(\alpha+\sigma_T) + mg\cos\gamma\right) + q \quad (2)$$

$$\dot{\theta} = q \quad (3)$$

$$\dot{q} = \frac{1}{I_y}\left(M + T_n l_{tz}\cos\sigma_T\right) \quad (4)$$

where $V_{tas}, \alpha, \theta, q, \gamma$ represent true air speed, angle of attack, pitch angle, pitch rate and flight path angle respectively. The parameters in (1)-(4) are $m, g, I_y, T_n, l_{tz}, \sigma_T$ which represent mass, gravity, the body axis moment of inertia, total engine thrust, the distance from the engine centre line to the fuselage reference line and the engine inclination angle respectively.

Define the state vector $x = \text{col}(V_{tas}, \alpha, \theta, q)$, then the drag force, lift force and pitch moments (D, L, M) from (1)-(4) can be written as:

$$D = \bar{q}SC_D(x,\delta) \quad (5)$$

$$L = \bar{q}SC_L(x,\delta) \quad (6)$$

$$M = \bar{q}S\bar{c}\left(C_m(x,\delta) + \Delta(x)\right) \quad (7)$$

where the dynamic pressure

$$\bar{q} = \frac{1}{2}\rho V_{tas}^2 \quad (8)$$

and $S, \bar{c}, \rho$ represent the wing area, wing mean aerodynamic chord and air density respectively. The dimensionless drag force, lift force and pitch moment coefficients $C_D(x,\delta), C_L(x,\delta)$ and $C_m(x,\delta)$ are functions of the states and control surface deflections, and are usually obtained through wind tunnel and flight tests. This data is then used to create an aerodynamic database in the form of a lookup table. For the RECOVER model, this data is available in [37]. The term $\Delta(x)$ in (7) represents unmodelled dynamics which are not considered during design, but which appear as part of the high fidelity model in RECOVER. This term is explicitly given by

$$\Delta(x) = -\frac{1}{\bar{c}}\left(C_D\sin\alpha + C_L\cos\alpha\right)\bar{x}_{cg} + \frac{\bar{c}\dot{\alpha}}{V_{tas}}\left(C_{m_{\dot{\alpha}}} - \frac{\bar{x}_{cg}}{\bar{c}}C_{L_{\dot{\alpha}}}\cos\alpha\right) \quad (9)$$

where $\bar{x}_{cg} = x_{cg_{ref}} - x_{cg}$ represents the difference between the actual and the reference x-axis center of gravity [38]. In this paper it is assumed that $\Delta(x)$ is unknown.

A. Strict Feedback Form

To design the ISM scheme and the baseline backstepping control law, approximations will be made to the longitudinal aircraft dynamics in (1)-(4) to create a representation in 'strict feedback form' [39], [11]. Here, as in [11], the following simplifications are introduced:

- It is assumed that V_{tas} remains constant: i.e. $\dot{V}_{tas} \approx 0$. This can be achieved by introducing a separate feedback loop based on the measured speed and the auto throttle.
- As often argued in the flight dynamics literature (for example [40]), it is assumed that changes to the elevator mainly affect the pitch moment, and the effect on lift and drag can be neglected [11], [41] (i.e. $C_D(\delta) = 0, C_L(\delta) = 0$).
- In equation (2) $\dot{\alpha}$ can be replaced by $\gamma = \theta - \alpha$ (i.e flight path angle) to remove the dependency on the state q.

Using these approximations together with (5)-(7), the longitudinal dynamics in (1)-(4) for controller design purposes can be rewritten as

$$\dot{\gamma} = \frac{1}{mV_{tas}}\left(\bar{q}SC_L(x) + T_n\sin(\theta - \gamma + \sigma_T) - mg\cos\gamma\right) \quad (10)$$

$$\dot{\theta} = q \quad (11)$$

$$\dot{q} = \frac{1}{I_y}\left(\bar{q}S\bar{c}\left(C_m(x,\delta) + \Delta(x)\right) + T_n l_{tz}\cos\sigma_t\right) \quad (12)$$

In (10)-(12), the control surface deflection δ only appears in equation (12) and this allows many nonlinear schemes (e.g. backstepping and nonlinear dynamic inversion) to be used for control law design.

Note that (10)-(12) are only used for controller design, in the simulations the original equations (1)-(4) are used to test the design.

The pitch moment coefficient can be written in detail as functions of the states and control surfaces [40], [37]: specifically

$$C_m(x,\delta) = C_m(x) + \frac{dC_m}{d\delta_e}\delta_e + \frac{dC_m}{d\delta_s}\delta_s \quad (13)$$

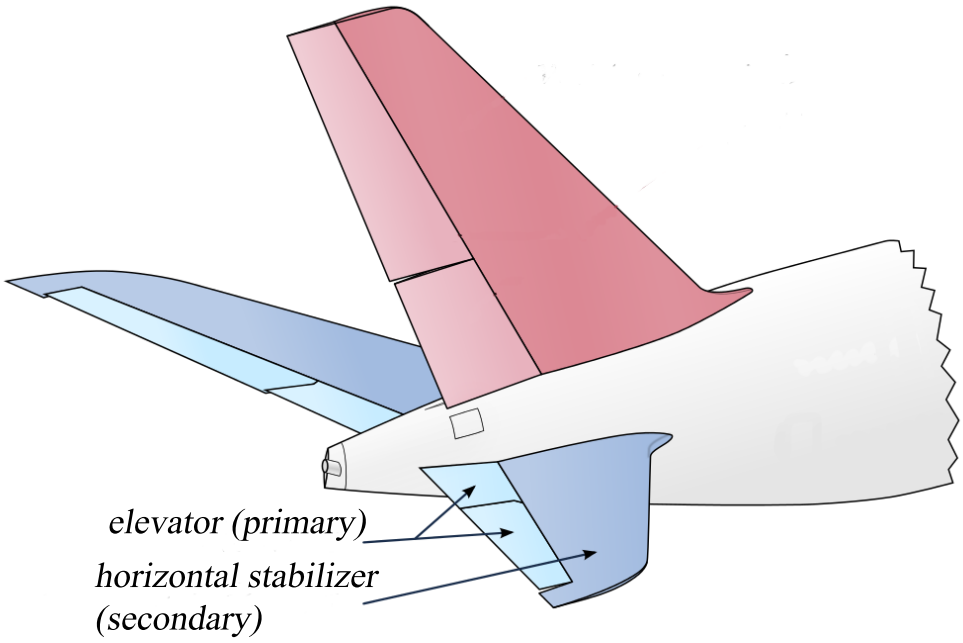

Fig. 1. elevator and stabilizer

where δ_e, δ_s are elevator and horizontal stabilizer deflections respectively. Combining equation (13) with equations (10)-(12), simplified equations of motion can be written in the form

$$\underbrace{\begin{bmatrix}\dot{\gamma}\\ \dot{\theta}\\ \dot{q}\end{bmatrix}}_{\dot{x}(t)} = \underbrace{\begin{bmatrix}\frac{1}{mV_{tas}}\left(\bar{q}SC_L(x) + T_n\sin(\alpha+\sigma_T) - mg\cos\gamma\right)\\ q\\ \frac{1}{I_y}\left(\bar{q}S\bar{c}C_m(x) + T_n l_{tz}\cos\sigma_t\right)\end{bmatrix}}_{f(x)} + \underbrace{\underbrace{\begin{bmatrix}0\\0\\ \frac{1}{I_y}\bar{q}S\bar{c}\frac{dC_m}{d\delta_e}\end{bmatrix}}_{g_e(x)} \;\Big|\; \underbrace{\begin{bmatrix}0\\0\\ \frac{1}{I_y}\bar{q}S\bar{c}\frac{dC_m}{d\delta_s}\end{bmatrix}}_{g_s(x)}}_{g(x)} \underbrace{\begin{bmatrix}\delta_e\\ \delta_s\end{bmatrix}}_{u(t)} + \underbrace{\begin{bmatrix}0\\0\\ \frac{1}{I_y}\bar{q}S\bar{c}\end{bmatrix}}_{b(x)}\Delta(x) \tag{14}$$

The vector $g_e(x)$ is associated with the primary control surface[1] (the elevator) [42]. Conversely the vector $g_s(x)$ is associated with the secondary control surface (the stabilizer) [42] which will be used when faults/failures occur on the primary control surface. (See Figure 1.)

Remark 1: Note that the term $\frac{dC_m}{d\delta_e}$ is assumed to be available either by online parameter estimation (e.g. [14]) or from a lookup table. In this paper the information is obtained from a lookup table based on [37]. However imprecision in the knowledge of $\frac{dC_m}{d\delta_e}$ will appear as matched uncertainty which will be suppressed by the sliding mode terms in the controller. The thrust T_n is also assumed to be available by converting engine pressure ratio (which is the commanded signal from the speed controller) into thrust through a lookup table which is also available in [37]. (Recall it is assumed speed is controlled by a separate "auto-throttle" control loop.)

To simplify the subsequent analysis, equation (14) can be written as

$$\begin{bmatrix}\dot{x}_1\\ \dot{x}_2\end{bmatrix} = \begin{bmatrix}f_1(x)\\ f_2(x)\end{bmatrix} + g(x)u(t) + b(x)\Delta(x) \tag{15}$$

[1]As defined on pages 4-5 in [42], the primary control surfaces are ones which move directly by the action of pilot input for pitch, roll and yaw control. These affect motion about the transverse, longitudinal and normal axes. The secondary control surfaces e.g. stabilizer, are primarily used to trim the aircraft, but can also be used to change pitch motion in the event of an emergency [19], [43].

where the state sub-vector $x_1 = \text{col}(\gamma, \theta)$ and $x_2 = q$. The input distribution vector

$$g(x) = \left[\begin{array}{c|c} g_e(x) & g_s(x) \end{array} \right] = \left[\begin{array}{c|c} 0_{2\times 1} & 0_{2\times 1} \\ g_1(x) & g_2(x) \end{array} \right] \tag{16}$$

where $g_1(x) = \frac{1}{I_y}\bar{q}S\bar{c}\frac{dC_m}{d\delta_e}$ and $g_2(x) = \frac{1}{I_y}\bar{q}S\bar{c}\frac{dC_m}{d\delta_s}$. The disturbance matrix $b(x)$ in (14) can be written as

$$b(x) = \left[\begin{array}{c} 0_{2\times 1} \\ b_1(x) \end{array} \right] \tag{17}$$

where $b_1(x) = \frac{1}{I_y}\bar{q}S\bar{c}$.

III. Control Law Development

Consider the effect of faults on each actuator modelled by

$$u_i^e(t) = w_i(t)u_i(t) + \xi(t) \quad \text{for } i = 1, 2 \tag{18}$$

where the scalars $0 \leq w_i(t) \leq 1$, and $\xi(t)$ is an exogenous signal. Here $u_i^e(t)$ represents the effective control signal which influences the aircraft dynamics, taking into account the detrimental impact of the fault. The scalars $w_1(t)$ and $w_2(t)$ are the so-called control surface effectiveness gains associated with the primary (elevator) and secondary (stabilizer) control surfaces respectively. If $w_i = 1$, the corresponding ith control surface is working perfectly, while $w_i = 0$ indicates a total failure. If $0 < w_i < 1$, a partial fault is present in the ith control surface. Ignoring the term $\xi(t)$ which does not effect stability[2], the system in (15) subject to potentially faulty actuators can be written in the form

$$\left[\begin{array}{c} \dot{x}_1 \\ \dot{x}_2 \end{array} \right] = \left[\begin{array}{c} f_1(x) \\ f_2(x) \end{array} \right] + \left[\begin{array}{cc} 0_{2\times 1} & 0_{2\times 1} \\ g_1(x) & g_2(x) \end{array} \right] W(t)u(t) + b(x)\Delta(x) \tag{19}$$

where the matrix $W(t) = \text{diag}(w_1(t), w_2(t))$.

For simplicity, factorize $g(x)$ so that (15) can be written as

$$\left[\begin{array}{c} \dot{x}_1 \\ \dot{x}_2 \end{array} \right] = \left[\begin{array}{c} f_1(x) \\ f_2(x) \end{array} \right] + g_1(x) \left[\begin{array}{cc} 0_{2\times 1} & 0_{2\times 1} \\ 1 & g_2^s(x) \end{array} \right] W(t)u(t) + b(x)\Delta(x) \tag{20}$$

where

$$g_2^s(x) = \frac{g_2(x)}{g_1(x)} \tag{21}$$

For the aircraft example considered here, $g_1(x)$ and $g_2(x)$ are both nonzero since $\frac{dC_m}{d\delta_e} \neq 0$ and $\frac{dC_m}{d\delta_s} \neq 0$ for typical regions in the flight envelope as shown in Figure 2(a) and 2(b). The data in Figure 2(a) and 2(b) has been extracted from RECOVER [43] and [37], and guarantees the inverse in (21) exists and the system (20) is controllable when faults/failures occur to the elevator. (Note that the maximum ceiling is 45,000ft and maximum level speed is Mach 0.895 at 30000ft).

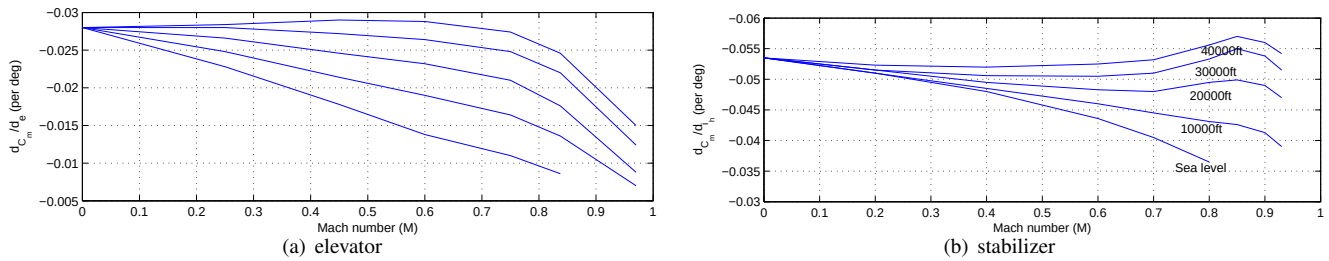

(a) elevator (b) stabilizer

Fig. 2. pitching moment coefficient due to elevator and stabilizer deflections [43], [37]

[2]Although of course it has a detrimental impact on performance, since it acts as an external disturbance to the post-fault system.

A. Nominal Back-Stepping Control Law

Assume that for the nominal system

$$\dot{x}(t) = f(x) + g_e(x)u_0(t) \tag{22}$$

a controller

$$u_0(x) = \mathcal{K}(x) \tag{23}$$

has been designed using the primary control surface such that the nominal closed system

$$\dot{x}(t) = f(x) + g_e(x)\mathcal{K}(x) \tag{24}$$

is stable. In this paper, the baseline controller for the elevator is given by a backstepping control scheme whose structure was originally proposed in [11], [34]. Specifically here

$$u_0(t) = \mathcal{K}(x) = \left(\frac{dC_m}{d\delta_e}\right)^{-1}\left(\frac{I_y\dot{q}_{des} - \bar{q}S\bar{c}C_m(x) - T_n l_{tz}\cos\sigma_t}{\bar{q}S\bar{c}}\right) \tag{25}$$

where

$$\dot{q}_{des} = -\begin{bmatrix} \kappa_1\kappa_2\kappa_3 & \kappa_2\kappa_3 & \kappa_3 \end{bmatrix}\begin{bmatrix} \gamma - \gamma_{ref} \\ \theta - \gamma_{ref} - \alpha_0 \\ q \end{bmatrix} \tag{26}$$

where α_0 is the angle of attack at a steady state condition [34]. According to [34], the gains $\kappa_1, \kappa_2, \kappa_3$ must be chosen to satisfy

$$\begin{aligned} \kappa_1 &> -1 \\ \kappa_2 &> 0 \\ \kappa_3 &> \begin{cases} \kappa_2 & \text{if } \kappa_1 \le 0 \\ \kappa_2(1+k_1) & \text{if } \kappa_1 > 0 \end{cases} \end{aligned} \tag{27}$$

For details of this backstepping controller, see [11], [34].

B. Control Allocation

Consider the situation when the actuator effectiveness gains w_1 and w_2 are not perfectly known. Their estimates $\hat{w}_1$ and $\hat{w}_2$ are assumed to be computed by a fault detection and isolation (FDI) scheme (which is required for the approach proposed in this paper). Consequently, as part of the estimation process, and by 'clipping' the estimates arising from the calculations if necessary, it can be assumed that they satisfy $0 \le \hat{w}_1(t) \le 1$ and $0 < \hat{w}_2(t) \le 1$ if they are to represent realistic effectiveness levels. However, these estimates my not be perfect, and so for analysis purposes it is assumed that they are related to the real values w_1 and w_2 according to

$$\underbrace{\begin{bmatrix} w_1(t) & 0 \\ 0 & w_2(t) \end{bmatrix}}_{W(t)} = \underbrace{\begin{bmatrix} \hat{w}_1(t) & 0 \\ 0 & \hat{w}_2(t) \end{bmatrix}}_{\widehat{W}(t)}\begin{bmatrix} 1+\delta_1(t) & 0 \\ 0 & 1+\delta_2(t) \end{bmatrix} = \begin{bmatrix} \hat{w}_1(t)(1+\delta_1(t)) & 0 \\ 0 & \hat{w}_2(t)(1+\delta_2(t)) \end{bmatrix} \tag{28}$$

In (28) the scalars $\delta_1(t), \delta_2(t)$ represent imperfections in the estimations and are assumed to satisfy

$$\delta_{\min} \le \delta_1(t), \delta_2(t) \le \delta_{\max} \tag{29}$$

where $\delta_{\min}, \delta_{\max}$ are known scalars and $\max\{|\delta_{\min}|, |\delta_{\max}|\} < 1$. The expressions in (28) ensure that the true values of the effectiveness levels

$$w_i(t) \in \begin{bmatrix} \hat{w}_i + \delta_{min}\hat{w}_i, & \hat{w}_i + \delta_{max}\hat{w}_i \end{bmatrix} \tag{30}$$

and importantly, since $\delta_{min} > -1$, (30) guarantees $w_i(t) \geq 0$. Note that (30) is a *conservative bound* since there is no guarantee that $\hat{w}_i + \delta_{max}\hat{w}_i \leq 1$. Consequently, from a mathematical perspective the proofs in the paper demonstrate that the scheme will work for values of $w_i(t) > 1$; although $w_i > 1$ is an unrealistic/unobtainable situation from an engineering perspective. Based on (28), equation (20) can be written as

$$\begin{bmatrix} \dot{x}_1 \\ \dot{x}_2 \end{bmatrix} = \begin{bmatrix} f_1(x) \\ f_2(x) \end{bmatrix} + g_1(x) \begin{bmatrix} 0_{2\times 1} & 0_{2\times 1} \\ 1 & g_2^s(x) \end{bmatrix} \begin{bmatrix} \hat{w}_1(t)(1+\delta_1(t)) & 0 \\ 0 & \hat{w}_2(t)(1+\delta_2(t)) \end{bmatrix} u(t) + b(x)\Delta(x) \tag{31}$$

For the potentially faulty system in (31), consider as a control law

$$u(t) = N(x) \underbrace{(\mathcal{K}(x) + \nu_n(t))}_{\nu(t)} \tag{32}$$

where the signal $\nu_n(t)$ is associated with the sliding mode component of the control law, and will be defined formally later in the paper. The 'control allocation matrix' $N(x)$ is given by

$$N(x) = \begin{bmatrix} 1 \\ \frac{1-\hat{w}_1(t)}{\hat{w}_2(t) g_2^s(x)} \end{bmatrix} \tag{33}$$

assuming $\hat{w}_2(t) \neq 0$ (i.e. assuming that the secondary control surface is failure free) and exploiting the fact that $g_2^s(x) \neq 0$.

Remark 2: Note that the control allocation matrix in (33) is different to the ones used in [20], [21]. Here the control allocation matrix is very bespoke and utilizes the specific aircraft equation of motion – especially the strict feedback form in (14).

Substituting (28) and (32)-(33) into (31) yields (after some straightforward algebra)

$$\underbrace{\begin{bmatrix} \dot{x}_1 \\ \dot{x}_2 \end{bmatrix}}_{\dot{x}(t)} = \underbrace{\begin{bmatrix} f_1(x) \\ f_2(x) \end{bmatrix}}_{f(x)} + \left(\underbrace{\begin{bmatrix} 0_{2\times 1} \\ g_1(x) \end{bmatrix}}_{g_e(x)} + \underbrace{\begin{bmatrix} 0_{2\times 1} \\ g_1(x)\hat{\delta}(t) \end{bmatrix}}_{\hat{g}_e(x)} \right) \underbrace{(\mathcal{K}(x) + \nu_n(t))}_{u(t)} + \underbrace{\begin{bmatrix} 0_{2\times 1} \\ b_1(x) \end{bmatrix}}_{b(x)} \Delta(x) \tag{34}$$

where

$$\hat{\delta}(t) := (\hat{w}_1(t)\delta_1(t) + (1 - \hat{w}_1(t))\delta_2(t))) \tag{35}$$

Since by assumption $0 \leq \hat{w}_1(t) \leq 1$, it follows that $\hat{\delta}(t) \in \begin{bmatrix} \delta_1(t) & \delta_2(t) \end{bmatrix}$ (i.e. it belongs to the line segments between the points δ_1 and δ_2), and therefore $\delta_{\min} \leq \hat{\delta}(t) \leq \delta_{\max}$.

Remark 3: Notice from equation (33) that during fault free conditions and actuator effectiveness is perfect $\widehat{W}(t) = W(t) = I_2$, and therefore $\hat{w}_1(t) = 1$, the control signal $u(t)$ becomes

$$u(t) = \begin{bmatrix} \mathcal{K}(x) + \nu_n(t) \\ 0 \end{bmatrix} \tag{36}$$

and thus only the primary control surfaces are used. In general if $\widehat{W}(t) \neq I$, then the lower component in (33) is nonzero and a control signal is sent to the secondary actuator.

C. Integral Sliding Modes

In this section, an expression for the control law component $\nu_n(t)$ in (32) will be developed. In particular this term will add robustness to the control allocation scheme proposed in Section III. This robustness will be introduced by the introduction of an integral sliding mode [44], [45]. Integral sliding modes are quite distinct from 'conventional' sliding modes [46]. In conventional sliding modes the order of the sliding motion is strictly reduced compared to the original order of the plant because of the 'dynamical collapse' induced by forcing the switching function to zero. In an ISM approach there is no reduction in order and the sliding motion is the order of the open-loop plant. This occurs because of the introduction of additional integrator dynamics at the time of design. In an ISM, the sliding motion is determined by the response of the ideal, uncertainty free

plant, under the control of a predetermined control law. The sliding mode element is thus viewed as a means of maintaining this ideal behaviour in the face of uncertainty.

Define a time-varying sliding surface as

$$\mathcal{S} = \{x \in \mathbb{R}^3 : \quad s(x,t) = 0\} \tag{37}$$

where

$$s(t) := Gx(t) - Gx(t_0) - G\int_{t_0}^{t} (f(x) + g_e(x)\mathcal{K}(x))d\tau \tag{38}$$

and $G \in \mathbb{R}^{1\times 3}$ is the design freedom. In this paper the gain will be chosen as

$$G := \left[\begin{array}{cc} 0_{1\times 2} & 1 \end{array} \right] \tag{39}$$

First it will be demonstrated that if a sliding motion occurs on $\mathcal{S}$ given in (37)-(38), then fault tolerance is achieved. Subsequently a control law $\nu(t)$, to achieve and maintain sliding will be proposed.

Proposition 1: If a sliding mode is maintained on $\mathcal{S}$ given by (37)-(38), then the associated sliding motion is governed by the stable system (24)-(25).

Proof: From the definition of G in (39), it follows that the scalar

$$Gg_e(x) = g_1(x) \neq 0, \; G\hat{g}_e(x) = g_1(x)\hat{\delta}(t), \; Gb(x) = b_1(x) \tag{40}$$

The fact that $Gg_e(x) \neq 0$ guarantees the existence of an unique equivalent control, and so the sliding mode control problem is well posed [47]. Taking the derivative of (38) along the trajectory of (31) and substituting from (34) yields

$$\begin{aligned} \dot{s}(x,t) &= G\dot{x}(t) - G(f(x) + g_e(x)\mathcal{K}(x)) \\ &= Gg_e(x)\nu_n(t) + G\hat{g}_e(x)(\mathcal{K}(x) + \nu_n(t)) + Gb(x)\Delta(x) \\ &= g_1(x)(1 + \hat{\delta}(t))\nu_n(t) + g_1(x)\hat{\delta}(t)\mathcal{K}(x) + b_1(x)\Delta(x) \end{aligned} \tag{41}$$

where $\nu_n(t)$ from (32) will be defined shortly to ensure a sliding motion on $\mathcal{S}$ can be maintained. During sliding $\dot{s} = s = 0$, and therefore since $g_1(x) \neq 0$ the 'equivalent control' [18] necessary to maintain sliding[3], is given by equating the left hand side of (41) to zero and solving the resulting algebraic equation to yield

$$\nu_{eq}(t) = -\left(g_1(x)\left(1 + \hat{\delta}(t)\right)\right)^{-1}\left(g_1(x)\hat{\delta}(t)\mathcal{K}(x) + b_1(x)\Delta(x)\right) \tag{42}$$

The equations of motion during the sliding mode can be obtained by substituting (42) into (34) to yield

$$\dot{x}(t) = f(x) + g_e(x)\mathcal{K}(x) \tag{43}$$

■

Remark 4: Note that equation (43) is the closed loop system associated with the baseline controller in (23), and that the unknown term $\Delta(x)$ does not appear. This is because $\Delta(x)$ is 'matched' uncertainty [18] and is therefore rejected by the sliding mode controller. Also note that G in (39) is not the surface advocated in [45] (which would be $G = (g_e^{\mathrm{T}}g_e)^{-1}g_e$). However, the choice in (39) means that the matrix G is fixed (not time varying) which simplifies the analysis. Furthermore since $(I - g_e(Gg_e)^{-1}G) = diag(1,1,0)$, the contraction properties discussed in [45] are still obtained since

$$\|I - g_e(Gg_e)^{-1}G\| = 1$$

(which is the minimum achievable value of the norm over all possible values of G).

[3]Note this is not the control law which is actually applied to the system, but represents an abstraction used to create an expression for the sliding motion: for details see [47].

The remainder of this section proposes a controller to ensure sliding can be achieved and maintained in the presence of faults, and formally demonstrates this is indeed the case.

Here, the sliding mode nonlinear term $\nu_n(t)$ is defined as

$$\nu_n(t) = -\varrho(x) g_1(x)^{-1} \text{sign}\left(s(x,t)\right) \quad \text{for } s(x,t) \neq 0 \tag{44}$$

where the modulation gain $\varrho(x)$ is any function satisfying

$$\varrho(x) > \frac{|g_1(x)|\,\bar{\delta}\,|\mathcal{K}(x)| + |b_1(x)||\Delta(x)| + \eta_0}{(1-\bar{\delta})} \tag{45}$$

where $\bar{\delta} = \max\{|\delta_{\min}|, |\delta_{\max}|\} < 1$ and η_0 is small positive scalar. Note: here $\bar{\delta}$ will be used as an user defined parameter employed to select the level of tolerance to the error in estimation of the effectiveness gains that the controller can tolerate.

Proposition 2: The control law given in (32), with the allocation matrix in (33), and the nonlinear injection term from (44)-(45), maintains a sliding motion provided $\bar{\delta} < 1$ and $w_2 \neq 0$.

Proof: Substituting from (44) into (41) yields

$$\dot{s}(x,t) \;\; = \;\; -\varrho(x)(1+\hat{\delta}(t))\text{sign}\left(s(x,t)\right) + g_1(x)\hat{\delta}(t)\mathcal{K}(x) + b_1(x)\Delta(x) \tag{46}$$

To show that sliding is maintained, consider a positive definite candidate Lyapunov function

$$V \;\; = \;\; \frac{1}{2}s^2 \tag{47}$$

It follows from (46) and (47) that

$$\dot{V} \;\; = \;\; -\varrho(x)(1+\hat{\delta}(t))|s(t)| + s(t)g_1(x)\hat{\delta}(t)\mathcal{K}(x) + s(t)b_1(x)\Delta(x) \tag{48}$$

Since

$$|\hat{\delta}(t)| < \bar{\delta} < 1 \tag{49}$$

using (49) and (45), equation (48) becomes

$$\begin{aligned} \dot{V} \;\; &\leq \;\; |s(t)|\left(-\varrho(x)(1-|\hat{\delta}(t)|) + |g_1(x)|\,|\hat{\delta}(t)|\,|\mathcal{K}(x)| + |b_1(x)|\,|\Delta(x)|\right) \\ &\leq \;\; |s(t)|\left(-\varrho(x)(1-\bar{\delta}) + |g_1(x)|\,\bar{\delta}\,|\mathcal{K}(x)| + |b_1(x)|\,|\Delta(x)|\right) \\ &\leq \;\; -\eta_0|s(t)| = -\eta_0\sqrt{2}V^{1/2} \end{aligned} \tag{50}$$

This is sufficient to show that the 'reachability condition' [18] is satisfied and sliding is maintained. ■

The final control signal $u(t)$ which is supplied to all the available control surfaces (primary and secondary) is given by substituting (44) into (32) to yield

$$u(t) = \underbrace{\begin{bmatrix} 1 \\ \frac{1-\hat{w}_1(t)}{\hat{w}_2(t)g_2^s(x)} \end{bmatrix}}_{N(x)} \underbrace{\left(\mathcal{K}(x) - \varrho(x)g_1(x)^{-1}\text{sign}\left(s(t,x)\right)\right)}_{\nu_n(t)} \tag{51}$$

Remark 5: Note that (51) requires the estimates of actuator efficiency $\hat{w}_1$ and $\hat{w}_2$, but does not require knowledge of δ_1, δ_2 or $\Delta(x)$. The errors δ_1, δ_2 are only used in conjunction with $\hat{\delta}$ to prove sliding is maintained.

IV. SIMULATIONS

A. RECOVER benchmark model

For the design and analysis in this paper, a nonlinear model of a large transport aircraft, originally called FTLAB747, which has been used in the recent European GARTEUR FM-AG16 programme, will be considered. The model which runs under the Matlab and Simulink environment, has been extensively developed over many years by many different contributors (see for example [48], [49], [38] and more recently [50]) into a platform to test state of the art FTC and FDI schemes. In the recent European GARTEUR FM-AG16 programme [43], this model and its environment has been renamed 'RECOVER' and has been put forward as a benchmark platform to test and compare different state-of-the-art FTC schemes in the face of various types of actuator faults and failures. This includes a 'catastrophic failure' scenario based on the Bijlmermeer incident near Amsterdam in The Netherlands, which occurred in 1992 [51]. RECOVER now represents a high fidelity aircraft benchmark model based on rigid body dynamics with aerodynamic coefficients obtained from NASA through actual flight and wind tunnel tests. The model has 77 states and includes realistic sensors and actuator dynamics including hard nonlinearities representing limits on the rates and final positions of the actuators. See for example [50], [38] for details of the benchmark model.

All the simulations which follow have been conducted at a trim altitude of 2000m, a mass of 263 tonne, c.g. at 25% MAC, a speed of 92.6m/s and flap settings of 20deg. The modulation gain $\varrho(x)$ can be chosen based on worst case estimates of $|g_1(x)|$ and $|b_1(x)|$ in (45), obtained from graphs similar to those presented in Figure 2, together with bounds on $\Delta(t)$ in (9) using worst case bounds/estimates of the drag and lift coefficients C_D and C_L, together with the aerodynamic coefficients related to $\dot{\alpha}$. A possible structure for the modulation gain to satisfy (45) is

$$\varrho(x) = \varrho_2|\mathcal{K}(x)| + \varrho_1\|x\| + \varrho_0 \tag{52}$$

where the ϱ_i are positive constants: for an example of this approach see Chapter 3 in [18]. Here the gain from (44) has been simply chosen as $\varrho = 0.65$. This is very easy to implement and is shown to work well in simulation. This is in fact an aggressive choice for $\varrho(x)$ because the nonlinear term in (44) can contribute a signal in the range $[-0.65, 0.65]$ rad to the value of the overall virtual control signal because of the signum term. The units of the control signal are radians[4] and so this range represents a significant portion of the available/allowable control signal variation. It does however mean that significant errors in the estimation of $w_i(t)$ can be tolerated. Alternatively, at the cost of increasing the complication of the controller, an adaptive scheme [35] could be used for the modulation gain since in the fault free case 'compensation' by the sliding mode component is not required.

Remark 6: Although the term $\Delta(x)$ from (9) has been excluded from the design process, it appears in the high fidelity full nonlinear model used for simulation. As discussed in Section III-C, this will appear as matched uncertainty which will be suppressed by the sliding mode.

Note that an estimate of $W(t)$ from (15) can be obtained from any FDI scheme of choice. In large passenger aircraft, it is common to measure the actual control surface deflection for monitoring purposes [52]. Consequently, in this paper, it is assumed that $W(t)$ is estimated by comparing the measurement of control surface deflection and the command from the flight control system. In particular since any mismatch resulting from errors in the estimate of $W(t)$ used in the controller appears as matched uncertainty, the controller is able to compensate.

B. Outer loop control

In order to maintain V_{tas} at a setpoint during the simulations, a proportional-derivative (PD) based auto-throttle has been implemented as a separate loop. The corresponding proportional and derivative gains have been chosen as $K_{pVtas} = 1$ and

[4]although in all the plots they have been scaled and presented in terms of degrees because these units are more intuitive to most readers

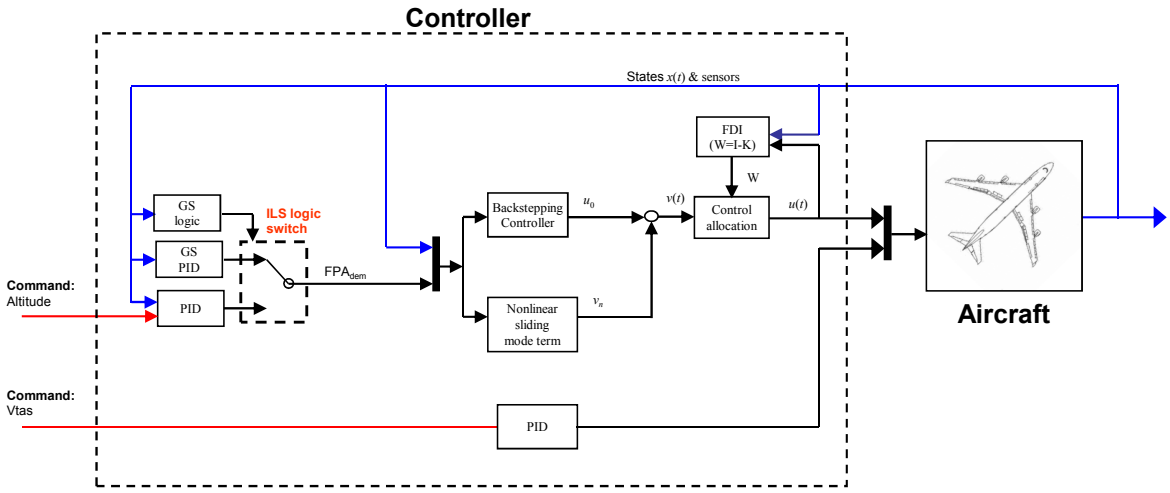

Fig. 3. Controller interconnection

$K_{d_{Vtas}} = 0.5$. An outer loop altitude control loop is also implemented as shown in Figure 3, to provide a flight path reference signal to the inner loop sliding mode-backstepping controller. This is based on a proportional-integral-derivative (PID) structure with gains $K_{p_{he}} = 0.001$, $K_{i_{he}} = 4 \times 10^{-5}$ and $K_{d_{he}} = 0.02$. Finally an Instrument Landing System (ILS) glideslope intercept and tracking facility is also included to create an automatic landing mode for the aircraft. This takes the form of a simple scalar feedback loop with proportional gain $K_{P_{GS}} = 7$.

In this paper, since only the longitudinal axis is considered, the Instrument Landing System (ILS) switches between an altitude/ flight path angle (FPA) command and glideslope[5] (GS) tracking (as shown in Figure 3). Specifically it changes the outer loop control from being pilot commanded (i.e. altitude demand tracking), to an automated landing mode using the GS signal. When the aircraft is inside the GS coverage zone, the GS controller will become active and provides the inner loop FPA command to the core longitudinal ISM controller, and no pilot input is required. This configuration can be found in all current large commercial aircraft in service (although the specific details of the outer-loop and inner-loop controller may differ). For details see Sections 11.8-11.10 in [42].

C. Results

The fault/failure cases and manoeuvres which are considered here are associated with the GARTEUR FM-AG16 benchmark scenarios [43]: specifically concerning the elevator. The simulation begins at a low speed and a low altitude (92.6m/s and 2000m). The aircraft starts to descend to 900m at 50sec and maintains altitude to intercept the ILS glideslope signal. Once the glideslope is intercepted, the aircraft descends at a commanded flight path angle of -3deg towards the runway. The flare (the last manoeuvre before touchdown) is not implemented in RECOVER and therefore the aircraft altitude is held at 50m above the runway. For consistency and for comparison, the actuator failures are set to occur at 100 sec.

For the simulations which follow, the gains of the back-stepping control law have been chosen as $\kappa_1 = 1$, $\kappa_2 = 0.6$ and $\kappa_3 = 3$. The control law (51) requires the estimates of actuator efficiency $\hat{w}_1$ and $\hat{w}_2$ which can be provided by a FDI scheme, or, more specifically by a fault estimation scheme. In this paper, it will be assumed that a measurement of the actual actuator deflection is available. As shown in [53], this is not an unrealistic assumption in aircraft systems. Using the same idea as in [35] (i.e. 'least squares' method), information provided by the actual actuator deflection is compared with the signals from the controller to provide estimates of the effectiveness of the actuators.

[5]The glideslope in the ILS provides vertical guidance to the aircraft during descent to the runway in order to provide an automated landing [19], [35]. The standard glide slope path demand is 3 deg. The glide slope signal is emitted by an antenna, located near the end of the runway and the glide slope provides the precise altitude required leading to the touchdown zone of the runway [19].

1) Elevator Float – imperfect $\widehat{W}$: Figure 4 shows the comparison between a fault free and the case when the elevator suffers a *float failure* [16] with imperfect estimation of the actuator effectiveness level $\widehat{W}$. A float failure corresponds to the control surface 'floating' about its zero moment position, thus becoming ineffective [16]. In the simulation, an elevator float is simulated by replacing the control signal by the angle of attack of the aircraft [16]. In terms of equation (18), this can be modelled as

$$u_1^e(t) = 0 + \alpha(t) \tag{53}$$

i.e where $w_1(t) = 0$ and $\xi(t) = \alpha(t)$. As a consequence the effective control signal $u_1^e(t)$ is completely disconnected from the command signal $u_1(t)$ generated by the control law. Figures 4(a) and 4(b) show that no degradation in the flight path angle, altitude and glideslope tracking performance occurs (all lines overlap) compared to the fault free case, despite the failure of the primary control surface and imperfect estimation of the actuator effectiveness level $\widehat{W}$. Figure 4(b) shows an altitude change command of 900m at 50 sec. The further altitude change to initiate tracking of the ILS glideslope is activated when the aircraft is within range of the ILS signal. Figure 4(b) shows the glide slope capture boolean signal equal to 1 to indicate GS capture. Once the ILS glideslope is activated at 448sec, the outerloop ILS controller provides the flight path command (of about -3deg in Figure 4(a)) forcing the glideslope deviation error to zero (Figure 4(b)). Figure 4(c) indicates the effect of an elevator float failure in which the control surface is unable to produce any pitching moment, and moves freely in the direction of the airflow. This can occur due to the loss of hydraulics for example. Once the failure occurs at 100 sec, as shown in Figure 4(c), the surface deflection becomes equal to the angle of attack of the aircraft [16] as shown in Figure 4(a). After the failure, the stabilizer becomes active and tries to compensate for the failed elevator. The effect of imperfect estimation can be seen in Figure 4(d), where even though the elevator has totally failed, the elevator effectiveness estimation $\hat{w}_1$ wrongly shows 50% effectiveness. Note that in the fault free case $w_1 = w_2 = 1$, but for simplicity, the lines are not labelled in Figure 4(d). Finally, Figure 4(d) also shows no visible degradation in the sliding mode performance when compared to the fault free case.

2) Elevator Lock in Place – imperfect $\widehat{W}$: Figure 5 shows the comparison between fault free and the case when an elevator jammed at a non-trim position (at 100sec), and in the presence of imperfect actuator effectiveness estimation $\widehat{W}$. The non-trim jam position creates an extra moment which needs to be compensated for. Note that the elevator jam is represented by

$$u_1^e(t) = 0 + u_1(t_f) \tag{54}$$

which in terms of (18) is associated with $w_1(t) = 0$ for all $t \geq t_f$ and $\xi(t) = u_1(t_f)$, where t_f (sec) is the time when the elevator failure occurs. Again this means for all $t \geq t_f$ the effective control signal $u_1^e(t)$ is decoupled from the command $u_1(t)$ determined by the control law. Figure 5(c) shows that once the elevator jams at 100sec, the stabilizer becomes active as the control signal is reallocated. The effect of the imperfect estimation can be seen in Figure 5(d). Here although the elevator has totally failed due to the lock in place failure, the elevator effectiveness estimation $\hat{w}_1$ wrongly shows 50% effectiveness. Again, as in Figure 4, despite the elevator jamming at a non-trim position, and imperfect estimation $\hat{w}_1$, Figures 4(a)-4(b) show no degradation in terms of all the tracking performance measures, compared to the fault free case.

3) Elevator Float: Backstepping control only – imperfect $\widehat{W}$: Figure 6 shows the comparison between the fault free case and when the elevator floats, using *only the baseline backstepping controller,* in the presence of imperfect actuator effectiveness estimation $\widehat{W}$. The same control allocation scheme as in Figures 4-5 has been considered to redistribute the control signal to the stabilizer. In comparison to the fault free condition, Figure 6(a) shows that the unmodelled term $\Delta(x)$ from (9) causes imperfect tracking of the flight path angle. When compared with the fault free condition, Figure 6(b) shows a small difference in terms of the altitude tracking as the imperfect flight path angle tracking has been compensated by the outer loop altitude control. Whereas in Figures 4(a)-4(b), the effect of the elevator failure and uncertainty has been totally compensated by the sliding mode, thus maintaining the same tracking performance as the fault free case.

V. Conclusions

This paper has proposed a fault tolerant scheme for longitudinal aircraft control. The scheme is designed directly from the nonlinear longitudinal equations of motion and incorporates an integral sliding mode control allocation scheme together with

a baseline backstepping control law for flight path angle tracking. In fault-free conditions only the primary control surface (the elevator) is used. However, when faults/failures occur, the integral sliding mode control allocation scheme is able to automatically provide robustness, and the control signals are redistributed to the redundant secondary control surfaces (the horizontal stabilizer). The control law has been tested on the RECOVER benchmark model which has been used in the GARTEUR AG16 programme for the study of FTC schemes. The simulations show that even in the presence of unmodelled dynamics (which have not been considered during the design process) excellent results are obtained for both nominal fault free and fault/failure scenarios. Future work aims to alleviate the strict feedback form in Section II-A, and remove the assumption that speed remains steady (all of which relate to the underlying back-stepping control law). In this paper, these coefficients are already available in the form of lookup tables, but future work will look into online parameter estimation in order to provide more accurate and current values. Although the scheme proposed in this paper is described specifically in terms of the longitudinal equations of motion of an aircraft, in principle, the underlying methodology can be applied to other systems controlled by a backstepping structure, provided that redundancy in the controls exists.

REFERENCES

[1] R. Patton, "Robustness in model-based fault diagnosis: the 1997 situation," *IFAC Annual Reviews*, vol. 21, pp. 101–121, 1997.

[2] Y. Zhang and J. Jiang, "Bibliographical review on reconfigurable fault-tolerant control systems," *Annual Reviews in Control*, vol. 32, pp. 229–252, 2008.

[3] M. Blanke, R. Izadi-Zamanabadi, S. A. Bogh, and C. P. Lunau, "Fault tolerant control systems - a holistic view," *Control Engineering Practice*, vol. 5, pp. 693–702, 1997.

[4] M. Verhaegen, S. Kanev, R. Hallouzi, C. Jones, J. Maciejowski, and H. Smail, "Fault tolerant flight control - a survey," in *Fault Tolerant Flight Control*, ser. Lecture Notes in Control and Information Sciences, C. Edwards, T. Lombaerts, and H. Smaili, Eds. Springer Berlin / Heidelberg, 2010, vol. 399, pp. 47–89.

[5] A. Marcos and G. J. Balas, "A robust integrated controller/diagnosis aircraft application," *International Journal of Robust and Nonlinear Control*, vol. 15, no. 12, pp. 531–551, 2005.

[6] S. Kanev and M. Verhaegen, "A bank of reconfigurable LQG controllers for linear systems subjected to failures," in *Proceedings of the 39th IEEE Conference on Decision and Control*, 2000, pp. 3684–9.

[7] Y. M. Zhang and J. Jiang, "Active fault-tolerant control system against partial actuator failures," *IEE Proceedings: Control Theory & Applications*, vol. 149, pp. 95–104, 2002.

[8] J. D. Bošković and R. K. Mehra, "A multiple model-based reconfigurable flight control system design," in *Proceedings of the 37th IEEE Conference on Decision and Control*, 1998, pp. 4503–8.

[9] J. M. Maciejowski and C. N. Jones, "MPC fault-tolerant control case study: flight 1862," in *Proceedings of the IFAC Symposium SAFEPROCESS '03, Washington*, 2003, pp. 119–124.

[10] T. Lombaerts, "Fault tolerant flight control: A physical model approach," Ph.D. dissertation, Delft University of Technology, 2010.

[11] O. Härkegård, "Backstepping and control allocation with applications to flight control," Ph.D. dissertation, Division of Automatic Control, Department of Electrical Engineering Linköping University, Sweden, 2003.

[12] Y. H. An, "A design of fault tolerant flight control systems for sensor and actuator failures using on-line learning neural networks," West Virginia University, Ph.D thesis, 1998.

[13] T. K. Vetter, S. R. Wells, and R. A. Hess, "Designing for damage–robust flight control design using sliding mode techniques," *Proceedings of the Institution of Mechanical Engineers, Part G: Journal of Aerospace Engineering*, vol. 217, pp. 245–261, 2003.

[14] T. J. J. Lombaerts, H. O. Huisman, Q. P. Chu, J. A. Mulder, and D. A. Joosten, "Flight control reconfiguration based on online physical model identification and nonlinear dynamic inversion," in *AIAA Guidance, Navigation and Control Conference and Exhibit*, no. AIAA 2008-7435, 2008.

[15] P. Goupil and A. Marcos, "Advanced Diagnosis for Sustainable Flight Guidance and Control: The European ADDSAFE Project," in *SAE AeroTech Congress & Exhibition*, no. doi:10.4271/2011-01-2804, 2011.

[16] S. Ganguli, A. Marcos, and G. J. Balas, "Reconfigurable LPV control design for Boeing 747-100/200 longitudinal axis," in *American Control Conference*, 2002, pp. 3612–3617.

[17] J. Shin, N. E. Wu, and C. Belcastro, "Adaptive linear parameter varying control synthesis for actuator failure," *Journal of Guidance, Control, and Dynamics*, vol. 27, pp. 787–794, 2004.

[18] C. Edwards and S. K. Spurgeon, *Sliding Mode Control: Theory and Applications*. Taylor & Francis, 1998.

[19] H. Alwi, C. Edwards, and C. P. Tan, *Fault Detection and Fault–Tolerant Control Using Sliding Modes*, ser. Advances in Industrial Control. Springer-Verlag, 2011.

[20] H. Alwi and C. Edwards, "Fault tolerant control using sliding modes with on-line control allocation," *Automatica*, vol. 44, no. 7, pp. 1859–1866, 2008.

[21] M. Hamayun, C. Edwards, and H. Alwi, "Design and analysis of an integral sliding mode fault tolerant control scheme," *IEEE Transactions on Automatic Control*, vol. 57, no. 7, pp. 1783–1789, 2012.

[22] V. Utkin and J. Shi, "Integral sliding mode in systems operating under uncertainty conditions," in *Proceedings of the 35th IEEE Conference on Decision and Control, CDC*, 1996, pp. 4591–4596.

[23] K. Nonaka and H. Sugizaki, "Integral sliding mode altitude control for a small model helicopter with ground effect compensation," in *Proceedings of the American Control Conference*, 2011.

[24] J. Wang, Q. Zong, B. Tian, and F. Wang, "Flight control for hypersonic vehicle based on quasi-continuous integral high-order sliding mode," in *24th Chinese Control and Decision Conference (CCDC)*, 2012.

[25] R. Zhang, C. Sun, J. Zhang, and Y. Zhou, "Second-order terminal sliding mode control for hypersonic vehicle in cruising flight with sliding mode disturbance observer," *Journal of Control Theory and Applications*, vol. 11, no. 2, pp. 299–305, 2013.

[26] Q. Hu and B. Xiao, "Adaptive fault tolerant control using integral sliding mode strategy with application to flexible spacecraft," *Journal of Control Theory and Applications*, vol. 44, no. 12, pp. 2273–2286, 2013.

[27] Q. Hu, Y. Zhang, X. H. Xinga, and B. Xiao, "Adaptive Integral-type Sliding Mode Control for Spacecraft Attitude Maneuvering Under Actuator Stuck Failures," *Chinese Journal of Aeronautics*, vol. 24, pp. 32–45, 2011.

[28] L. Peng, M. Jian-jun, L. Wen-qiang, and Z. Zhi-qiang, "Adaptive conditional integral sliding mode control for fault tolerant flight control system," in *7th International Conference on System Simulation and Scientific Computing*, 2008.

[29] M. Rubagotti, A. Estrada, F. Castanos, A. Ferrara, and L. Fridman, "Integral sliding mode control for nonlinear systems with matched and unmatched perturbations," *IEEE Transactions on Automatic Control*, vol. 56, no. 11, pp. 2699–2704, 2011.

[30] A. J. Koshkouei, A. S. I. Zinober, and K. J. Burnham, "Adaptive sliding mode backstepping control of nonlinear systems with unmatched uncertainty," *Asian Journal of Control*, vol. 6, no. 4, pp. 447–453, 2004.

[31] J. Davila, "Robust Backstepping Controller for Aircraft Dynamics," in *18th IFAC World Congress*, 2011.

[32] C. Edwards and I. Postlethwaite, "Anti-windup and bumpless-transfer schemes," *Automatica*, no. 2, pp. 199–210, 1998.

[33] M. C. Turner and D. J. Walker, "Linear quadratic bumpless transfer," *Automatica*, vol. 36, pp. 1089–1101, 2000.

[34] O. Härkegård and S. T. Glad, "A backstepping design for flight path angle control," in *Proceedings of the 39th IEEE Conference on Decision and Control, CDC*, 2000, pp. 3570–3575.

[35] H. Alwi, C. Edwards, O. Stroosma, and J. A. Mulder, "Fault tolerant sliding mode control design with piloted simulator evaluation," *AIAA Journal of Guidance, Control and Dynamics*, vol. 31, no. 5, pp. 1186–1201, 2008.

[36] ——, "Evaluation of a sliding mode fault-tolerant controller for the El Al incident," *AIAA journal of Guidance Control and Dynamics*, vol. 33, no. 3, pp. 677–694, 2010.

[37] C. Hanke and D. Nordwall, "The simulation of a jumbo jet transport aircraft. Volume II: Modelling data," NASA and The Boeing Company, Tech. Rep. CR-114494/D6-30643-VOL2, 1970.

[38] A. Marcos and G. J. Balas, "A Boeing 747–100/200 aircraft fault tolerant and diagnostic benchmark," Department of Aerospace and Engineering Mechanics, University of Minnesota, Tech. Rep. AEM–UoM–2003–1, 2003.

[39] R. Sepulchre, M. Jankovic, and P. Kokotovic, *Constructive Nonlinear Control*. Springer-Verlag, 1997.

[40] B. Etkin and L. D. Reid, *Dynamics of Flight: Stability and Control*. John Wiley & Sons, Inc., 1996.

[41] M. L. Steinberg and A. B. Page, "Nonlinear adaptive flight control with a backstepping design approach," in *AIAA Guidance, Navigation and Control Conference and Exhibit*, no. AIAA-1998-4230, 1998, pp. 728–738.

[42] D. Mclean, *Automatic Flight Control Systems*. Prentice-Hall, 1990.

[43] C. Edwards, T. Lombaerts, H. Smaili, and (Eds.), *Fault Tolerant Flight Control: A Benchmark Challenge*. Springer-Verlag: Lecture Notes in Control and Information Sciences, 2010, vol. 399.

[44] V. Utkin, J. Guldner, and J. Shi, *Sliding Mode Control in Electromechanical Systems*. Taylor & Francis, 1999.

[45] F. Castanos and L. Fridman, "Analysis and design of integral sliding manifolds for systems with unmatched perturbations," *IEEE Transactions on Automatic Control*, vol. 51, no. 5, pp. 853–858, 2006.

[46] Y. Shtessel, C. Edwards, L. Fridman, and A. Levant, *Sliding Mode Control and Observation*. Birkhauser, 2013.

[47] V. I. Utkin, *Sliding Modes in Control Optimization*. Springer-Verlag, Berlin, 1992.

[48] C. A. A. M. van der Linden, "DASMAT: Delft University aircraft simulation model and analysis tool," Technical University of Delft, the Netherlands, Tech. Rep. LR–781, 1996.

[49] M. H. Smaili, "Flight data reconstruction and simulation of EL AL Flight 1862," Delft University of Technology, Graduation Report, 1997.

[50] H. Smaili, J. Breeman, T. Lombaerts, and D. Joosten, "Recover: A benchmark for integrated fault tolerant flight control evaluation," in *Fault Tolerant Flight Control*, ser. Lecture Notes in Control and Information Sciences, C. Edwards, T. Lombaerts, and H. Smaili, Eds. Springer Berlin / Heidelberg, 2010, vol. 399, pp. 171–221.

[51] Anon, "El al flight 1862, aircraft accident report 92-11," Netherlands Aviation Safety Board, Hoofddorp, Tech. Rep., 1994.

[52] D. Brière, C. Favre, and P. Traverse, "A family of fault-tolerant systems: electrical flight controls, from Airbus A320/330/340 to future military transport aircraft," *Microprocessors and Microsystems*, pp. 75–82, 1995.

[53] D. Brière and P. Traverse, "Airbus A320/A330/A340 electrical flight controls: A family of fault-tolerant systems." *Digest of Papers FTCS-23 The Twenty-Third International Symposium on Fault-Tolerant Computing*, pp. 616–623, 1993.

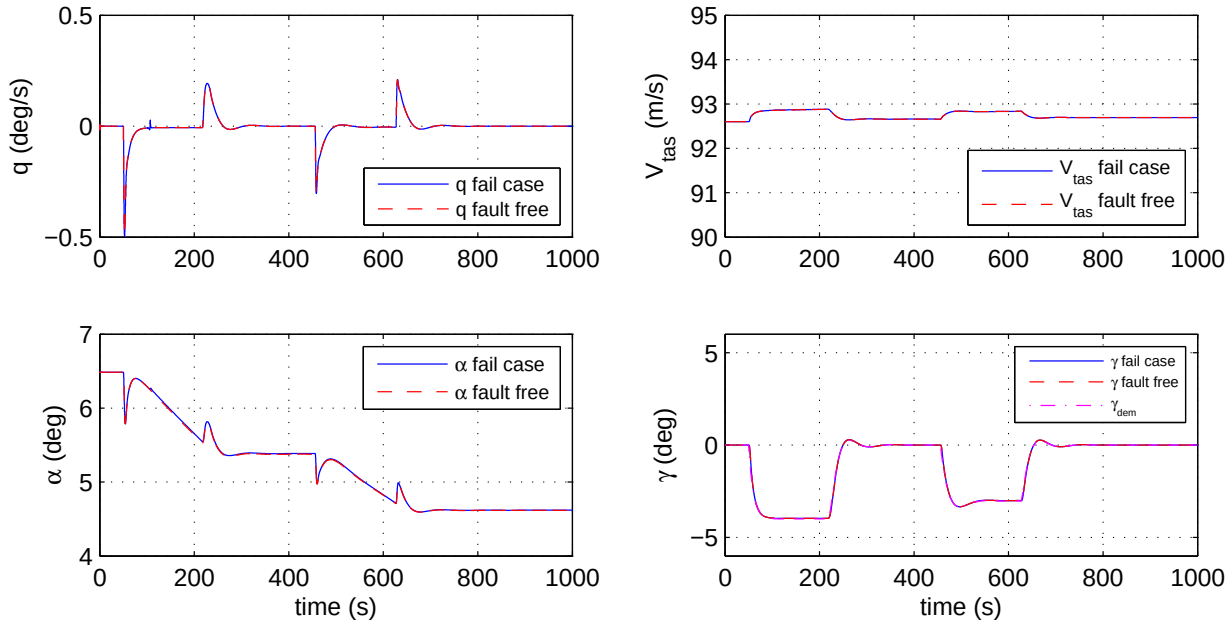

(a) states

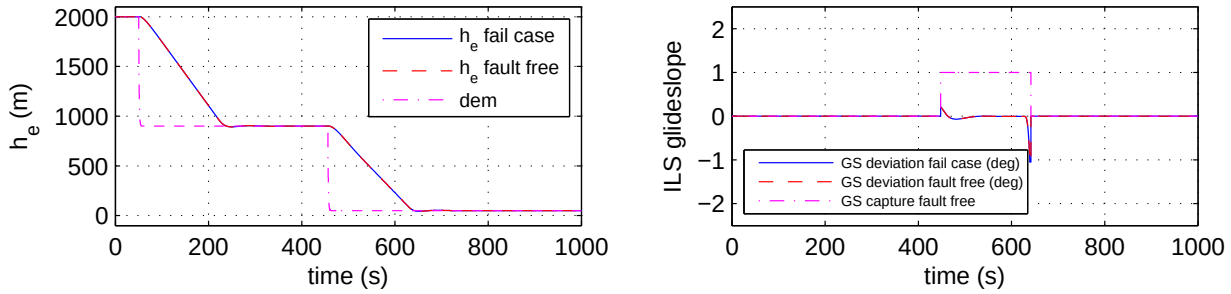

(b) altitude and ILS glideslope deviation

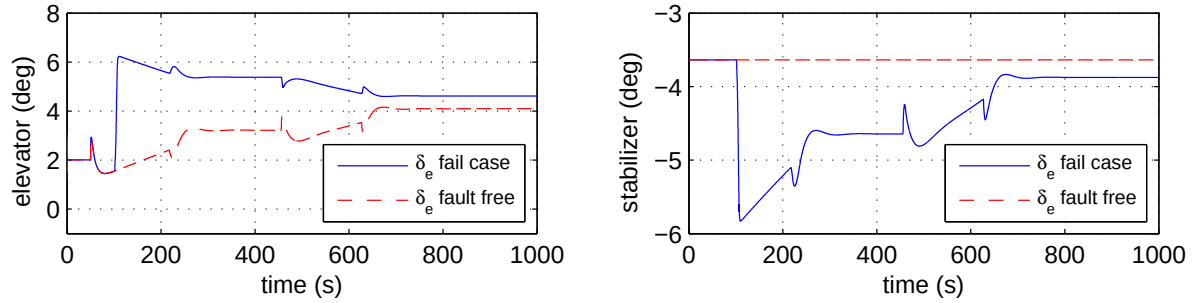

(c) control surface deflections

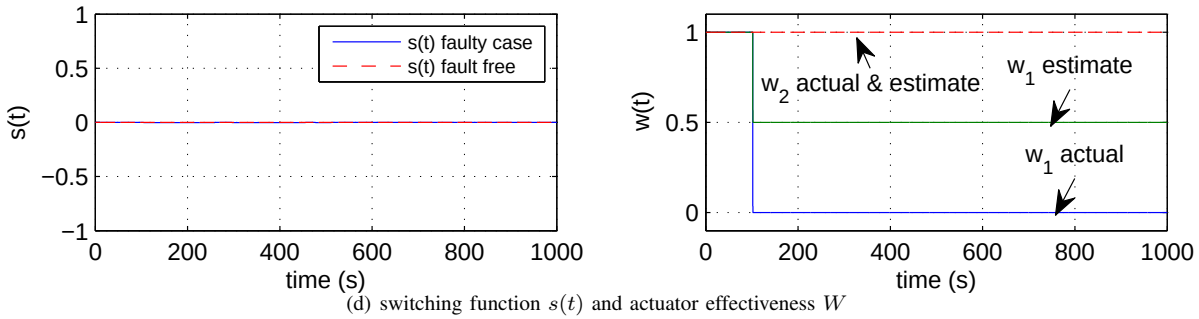

(d) switching function $s(t)$ and actuator effectiveness W

Fig. 4. elevator float performances – imperfect $\widehat{W}$

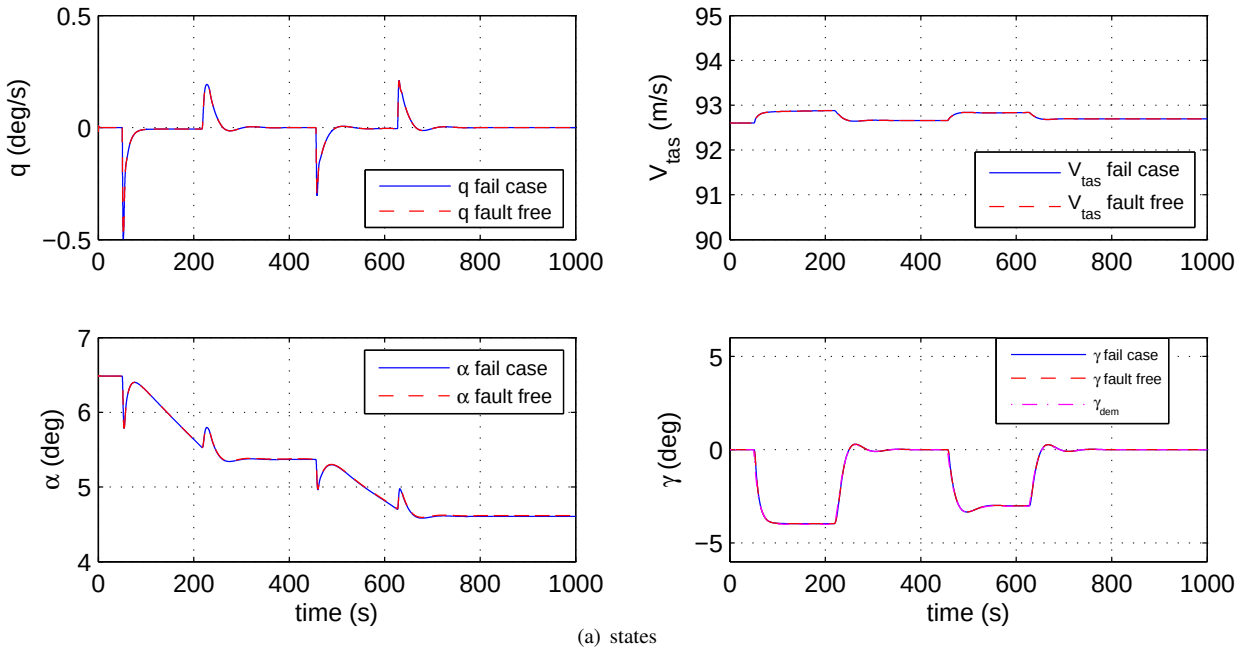

(a) states

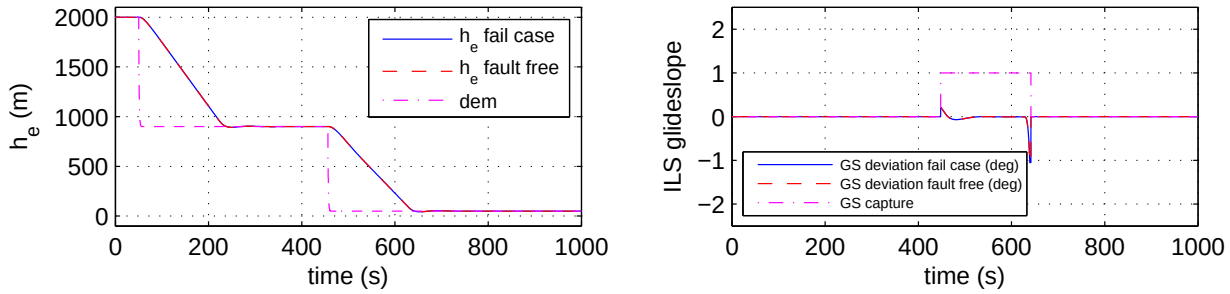

(b) altitude and ILS glideslope deviation

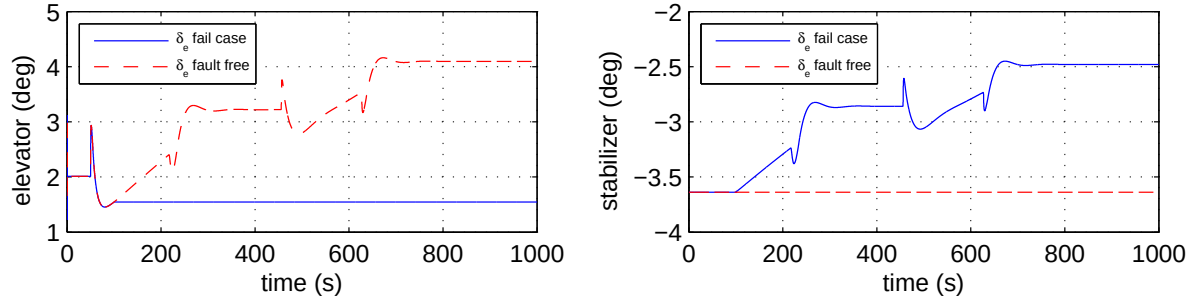

(c) control surface deflections

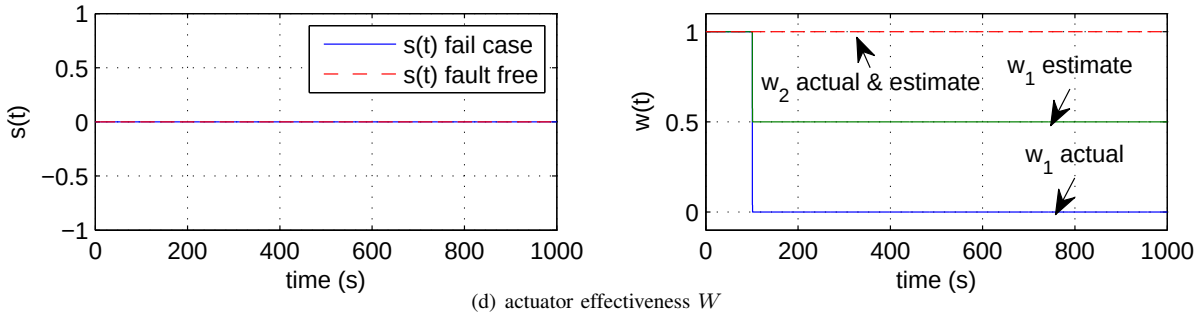

(d) actuator effectiveness W

Fig. 5. elevator lock in place performances – imperfect $\widehat{W}$

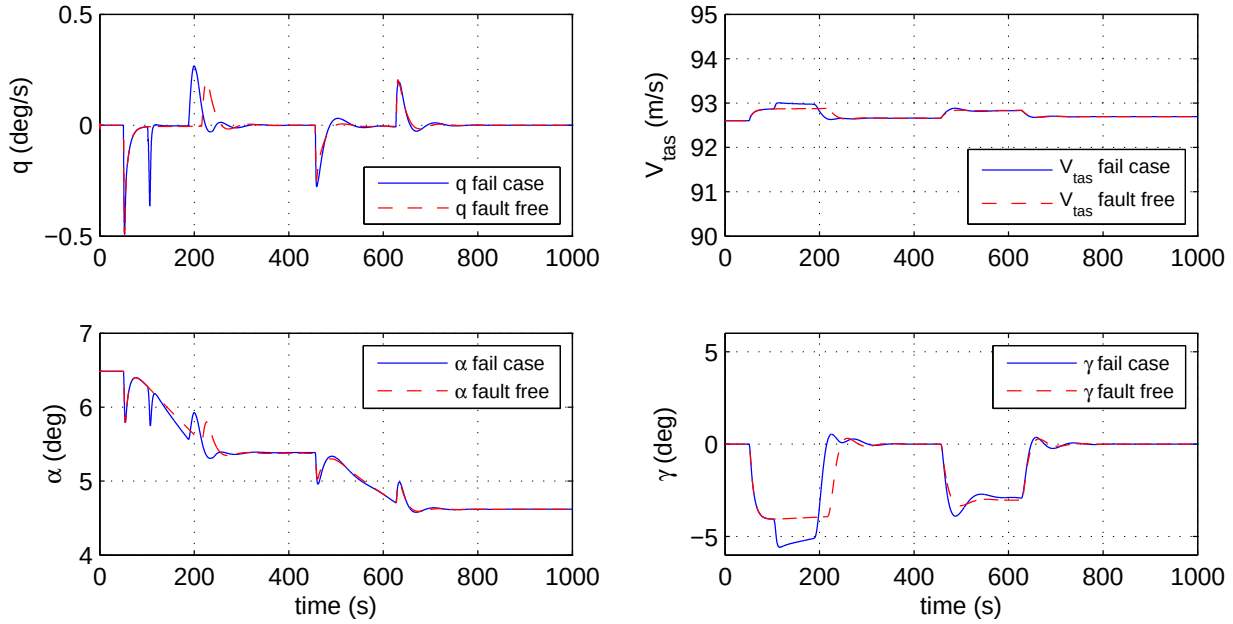

(a) states

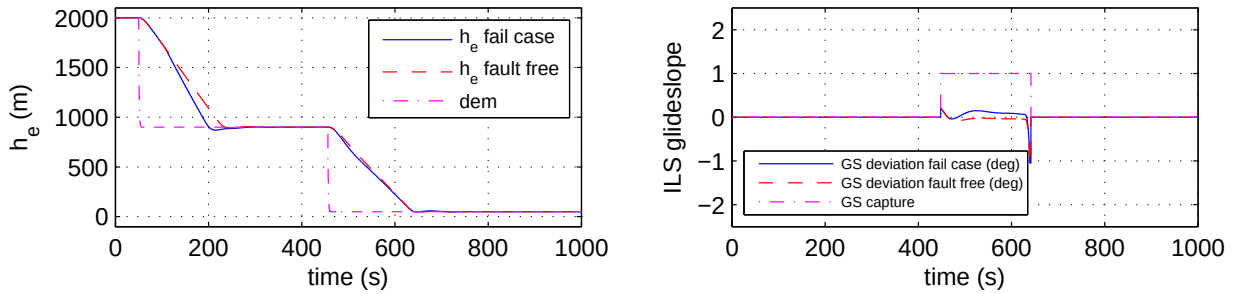

(b) altitude and ILS glideslope deviation

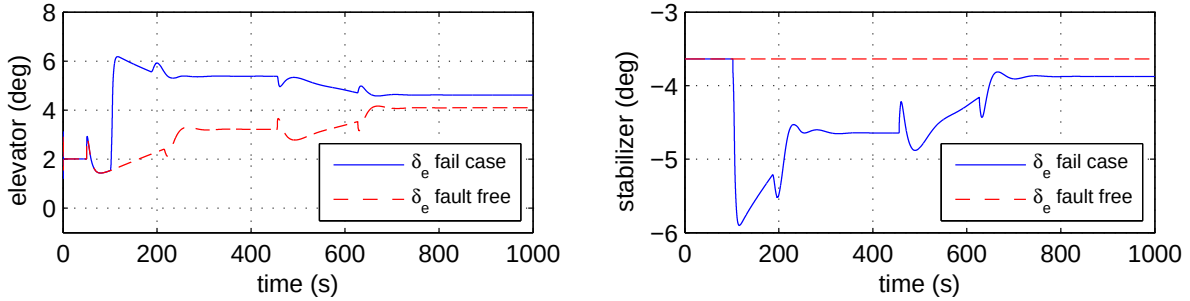

(c) control surface deflections

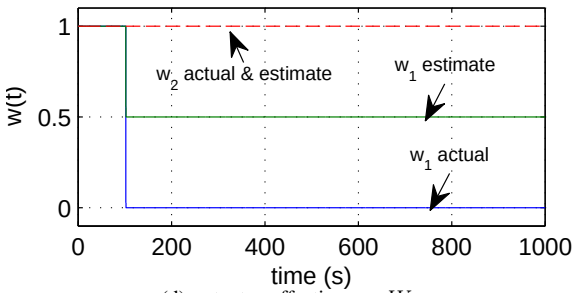

(d) actuator effectiveness W

Fig. 6. backstepping control only: elevator float performances – imperfect $\widehat{W}$